[CANCER RESEARCH 64, 934–941, February 1, 2004]

Basal Cell Carcinoma and Its Development: Insights from Radiation-Induced Tumors in *Ptch1*-Deficient Mice

Mariateresa Mancuso,[1] Simonetta Pazzaglia,[1] Mirella Tanori,[1] Heidi Hahn,[3] Paola Merola,[1] Simonetta Rebessi,[1] Michael J. Atkinson,[4] Vincenzo Di Majo,[1] Vincenzo Covelli,[2] and Anna Saran[1]

[1]Biotechnology Unit and [2]Radiation Protection Unit, ENEA-Ente per le Nuove Tecnologie, l'Energia e l'Ambiente, Centro Ricerche, Casaccia, Rome, Italy; [3]Institute of Human Genetics, University of Goettingen, Goettingen, Germany; and [4]Institute of Pathology, GSF-National Research Center for Environment and Health, Munich, Germany

ABSTRACT

Loss-of-function mutations in *Patched* (*Ptch1*) are implicated in constitutive activation of the Sonic hedgehog pathway in human basal cell carcinomas (BCCs), and inherited *Ptch1* mutations underlie basal cell nevus syndrome in which a typical feature is multiple BCC occurring with greater incidence in portals of radiotherapy. Mice in which one copy of *Ptch1* is inactivated show increased susceptibility to spontaneous tumor development and hypersensitivity to radiation-induced tumorigenesis, providing an ideal *in vivo* model to study the typical pathologies associated with basal cell nevus syndrome. We therefore examined BCC development in control and irradiated *Ptch1*$^{neo67/+}$ mice. We show that unirradiated mice develop putative BCC precursor lesions, *i.e.*, basaloid hyperproliferation areas arising from both follicular and interfollicular epithelium, and that these lesions progress to nodular and infiltrative BCCs only in irradiated mice. Data of BCC incidence, multiplicity, and latency support the notion of epidermal hyperproliferations, nodular and infiltrative BCC-like tumors representing different stages of tumor development. This is additionally supported by the pattern of p53 protein expression observed in BCC subtypes and by the finding of retention of the normal remaining *Ptch1* allele in all nodular, circumscribed BCCs analyzed compared with its constant loss in infiltrative BCCs. Our data suggest chronological tumor progression from basaloid hyperproliferations to nodular and then infiltrative BCC occurring in a stepwise fashion through the accumulation of sequential genetic alterations.

INTRODUCTION

Basal cell carcinoma (BCC) is the most common skin cancer, accounting for ~70% of all skin malignancies. The actual risk of metastasis for these tumors is exceedingly rare, but they are locally aggressive, and 5–9% may have multiple recurrences (1). Although the majority of BCCs arise sporadically, several cases are attributable to the basal cell nevus syndrome (BCNS), an autosomal dominantly inherited disorder characterized by the occurrence of multiple BCCs and of extracutaneous tumors (2). Genetic studies on patients with BCNS have led to the identification of inactivating mutations in the human homologue of the *Drosophila* gene *Ptch1* as the genetic defect underlying this syndrome (3, 4). This tumor suppressor gene is also inactivated in sporadic BCCs (5).

Ptch1 is a transmembrane protein that together with Smoothened forms a receptor complex for Shh. The Ptch1 protein is expressed in the cell membrane of target tissues, where it represses Smoothened signaling. Binding of Shh to Ptch1 (physiological activation) or mutational inactivation of Ptch1 (pathological activation) suspends the inhibition of Smoothened, which results in the activation of the hedgehog pathway (6). Mutations in other genes of the pathway are also involved in the genesis of BCC. *Smoothened*-activating mutations have been found in 21% of sporadic BCCs and transgenic mice overexpressing mutant *Smoothened* develop skin abnormalities similar to BCCs (7–9). Moreover, Oro *et al.* (10) showed that transgenic mice overexpressing *Shh* in the skin develop many features of BCNS, demonstrating that *Shh* overexpression is sufficient to induce BCC in mice.

Shh and its receptor complex have been shown to be expressed during many processes of embryonic development. In particular, during hair follicle morphogenesis, *Shh* expression correlates with hair follicle formation. A similar role for Shh signaling has been identified in the postnatal hair follicle, where its up-regulation has been recognized as a biological switch that induces resting hair follicles to enter anagen, the phase of active hair growth (11). Although its origin is still debated, BCC has been described classically as a follicular tumor (12).

Mice in which one copy of *Ptch1* is inactivated provide an ideal *in vivo* model to study the typical pathologies associated with BCNS. Two independent mouse lines heterozygous for *Ptch1* have recently been generated through targeted disruption of exons 6 and 7 (13) or exons 1 and 2 (14). Analogously to BCNS patients, both mouse strains show an increased susceptibility to spontaneous tumor development (medulloblastomas and rhabdomyosarcomas) and hypersensitivity to ionizing radiation-induced tumorigenesis. In a previous study, in fact, we reported a strong enhancement of medulloblastoma development after neonatal X-ray irradiation of *Ptch1*$^{neo67/+}$ heterozygotes (15). Regarding cutaneous tumorigenesis, Aszterbaum *et al.* (16) reported a strong enhancement of BCC tumorigenesis after chronic UV exposure of *Ptch1*$^{+/-}$ (exon 1/2) mice and the appearance of microscopically detectable trichoblastoma-like tumors after exposure to a single dose of ionizing radiation. Enhancement of brain and skin tumors by ionizing radiation in mice lacking one *Ptch1* copy suggests that additional genetic lesions are required for oncogenic transformation.

This study was carried out to additionally clarify the mechanisms of ionizing radiation-induced BCC tumorigenesis in *Ptch1* heterozygous knockout mice generated through disruption of exons 6–7 (*Ptch1*$^{neo67/+}$). To this aim, we used animals that were irradiated with various modalities and at different ages and followed for their entire life span. Here, we report the induction of both microscopically (nodular subtype) and macroscopically (infiltrative subtype) detectable BCCs after exposure of *Ptch1*$^{neo67/+}$ mice to a single dose of X-rays, providing evidence of a direct causal relationship between exposure to *ionizing radiation* and BCC tumorigenesis. Our data demonstrate that this mouse model recapitulates the etiology and the histopathology of the human disease. Moreover, by examining the pattern of p53 protein expression and loss of heterozygosity at the *Ptch1* locus in the histopathological variants of BCC, we provide new insights into the molecular bases of BCC development.

MATERIALS AND METHODS

Animals. Mice lacking one *Ptch1* allele, generated through targeted disruption of exons 6 and 7 in 129/SV ES cells and maintained on CD1 background, were used for this study. *Ptch1*$^{neo67/+}$ mice were genotyped using PCR

Received 8/7/03; revised 10/6/03; accepted 11/17/03.

Grant support: [1]This work was partially supported by the Commission of the European Communities under Contract FIGH-CT-1999-00006 and by Progetto Strategico 1998 (L. 449/97-MURST).

The costs of publication of this article were defrayed in part by the payment of page charges. This article must therefore be hereby marked *advertisement* in accordance with 18 U.S.C. Section 1734 solely to indicate this fact.

Note: M. Mancuso and S. Pazzaglia contributed equally to this work.

Requests for reprints: Anna Saran, Biotechnology Unit, ENEA CR-Casaccia, Via Anguillarese 301, 00060 Rome, Italy. Phone: 39-06-30484304; Fax: 39-06-30483644; E-mail: saran@casaccia.enea.it.

Table 1 *Experimental groups*

Dose and irradiation modality	Age at irradiation (days)	*Ptch1* genotype	No. of mice
3 Gy whole body	4	+/+	46
		+/−	52
3 Gy whole body	90	+/+	40
		+/−	39
4 Gy local	60	+/+	56
		+/−	61
None		+/+	52
		+/−	52

primers specific for the neo insert and wild-type sequences as described previously (13). Animals were housed under conventional conditions with food and water available *ad libitum* and a 12-h light cycle. The experimental protocols were reviewed by the Institutional Animal Care and Use Committee.

Treatment. X-ray irradiation (HVL = 1.6 mmCu) was performed using a Gilardoni CHF 320G X-ray generator (Gilardoni S.p.A.; Mandello del Lario, Lecco, Italy) operated at 250 kVp, 15 mA, with filters of 2.0 mm of Al and 0.5 mm of Cu. *Ptch1*$^{neo67/+}$ mice and wild-type littermates of both sexes were whole-body irradiated with 3 Gy of X-rays as newborns (4 days) or adults (90 days).

In addition, 2-month-old mice were subjected to local irradiation of the dorsal skin with a single dose of 4 Gy of X-rays. Briefly, anesthetized mice were radially positioned on a lead plate, and shaped lead shields were placed on each mouse to provide protection to the body parts to be spared. A dorsal skin area of 3 cm^2 was irradiated through a central trapezoidal window of a lead shield (4-mm thickness, 60 mm in length). The shield was accurately positioned on the anesthetized mouse using its tail insertion as reference. The irradiation modalities and size of experimental groups are summarized in Table 1. In total, the present study involved irradiation of 152 heterozygotes and 142 wild-type littermates. Groups of 52 heterozygous and 52 wild-type mice were left untreated as controls.

Histological Analysis and Tumor Quantification. Mice were inspected daily and at the first sign of morbidity or when tumors were visible were sacrificed and complete autopsies performed. A piece of grossly normal appearing dorsal skin with an area of 5 cm^2, corresponding to the site of local irradiation or an equivalent area of macroscopic-tumor-bearing skin, was fixed in 4% buffered formalin. Paraffin sections (7-μm thick) were analyzed after staining with H&E. In several instances, animals died without appearing moribund. These animals were also necropsied, but autolysis of the tissues prevented accurate histopathology. Thus, they were not included in our results. Tumor incidence was expressed as the percentage of mice with one or more infiltrative or nodular BCC-like tumors. For each group, tumor multiplicity was determined for nodular BCCs as the mean number of tumors (±SE) detected in groups of four heterozygotes at 60–90 weeks after irradiation. Briefly, three sections were collected from each mouse; to ensure a representative sampling, sections were recovered with an interval of 100 μm. Forty-five digital images/mouse, corresponding to 38 mm of transverse skin, were collected by IAS image-processing software (Delta Sistemi, Rome, Italy). The number of independent tumors in the skin analyzed (38 mm × 4) was averaged for calculation of tumor multiplicity.

Immunohistochemistry. Immunohistochemical analysis of skin samples from infiltrative or nodular BCCs was performed on paraffin sections (4-μm thick). Before incubation in 0.3% H_2O_2 in methanol for 30 min, sections were dewaxed, rehydrated, and pretreated by incubation in 0.1% trypsin in 0.1% $CaCl_2$ (pH 7.8) for 8–10 min at 37°C. Antibodies used in this study included rabbit polyclonal antibody against K14 (1:500 dilution; BabCo, Berkeley, CA), rabbit polyclonal antibody against p53 (1:500 dilution; Novocastra Laboratories, Newcastle, United Kingdom), and goat polyclonal antibody against Patched (G-19, 1:100 dilution; Santa Cruz Biotechnology, Santa Cruz, CA). Sections were incubated overnight at +4°C. Detection was carried out with the Vectastain Elite ABC Kit (Vector Laboratories, Inc., Burlingame, CA) by using rabbit or goat biotinylated secondary antibodies for 1 h at room temperature. After incubation with avidin-biotin immunoperoxidase, immunohistochemical staining was visualized with 3-amino-9-ethylcarbazole (Vector Novared kit; Vector Laboratories, Inc.), and slides were counterstained with hematoxylin.

Allelic Imbalance Analysis. Samples from infiltrative BCCs and noncancerous tissue were frozen at −80°C. Instead, microdissection of nodular BCC-like tumors was manually performed from paraffin sections (7 μm). Briefly, dewaxed and mildly stained slides were observed with a light microscope to identify nodular BCC areas. Microdissection was conducted using a small scalpel. DNA from each sample was extracted using the NucleoSpin Tissue kit (Macherrey-Nagel, Duren, Germany) and resuspended in 40 μl of deionized water. Amplification of *Ptch1* wild-type and targeted alleles was performed as described previously (15).

RESULTS

Survival after X-Ray Irradiation. The tumor-free survival of *Ptch1*$^{neo67/+}$ mice irradiated as adults was comparable with that of unirradiated heterozygotes. In contrast, a striking increase in mortality was observed in *Ptch1*$^{neo67/+}$ mice irradiated as newborns. At 28 weeks of age 80% of irradiated *Ptch1*$^{neo67/+}$ heterozygous had died compared with only 13% of unirradiated heterozygous mice (Fig. 1).

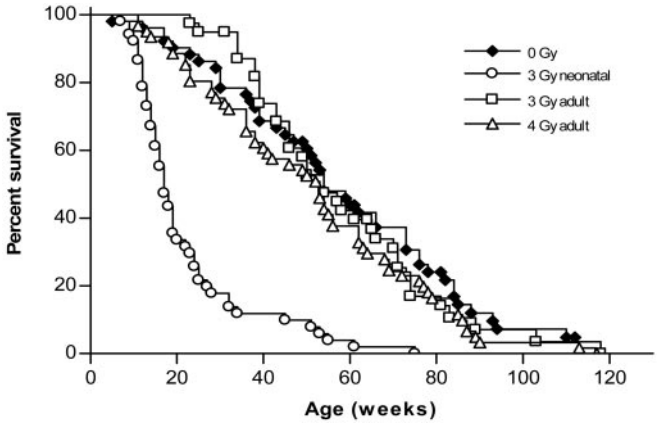

Fig. 1. Survival of *Ptch1*$^{neo67/+}$ heterozygous mice. No decrease in percent survival of mice irradiated as adults compared with *Ptch1* control mice was observed. In contrast, a striking decrease in survival was shown in mice irradiated as newborns.

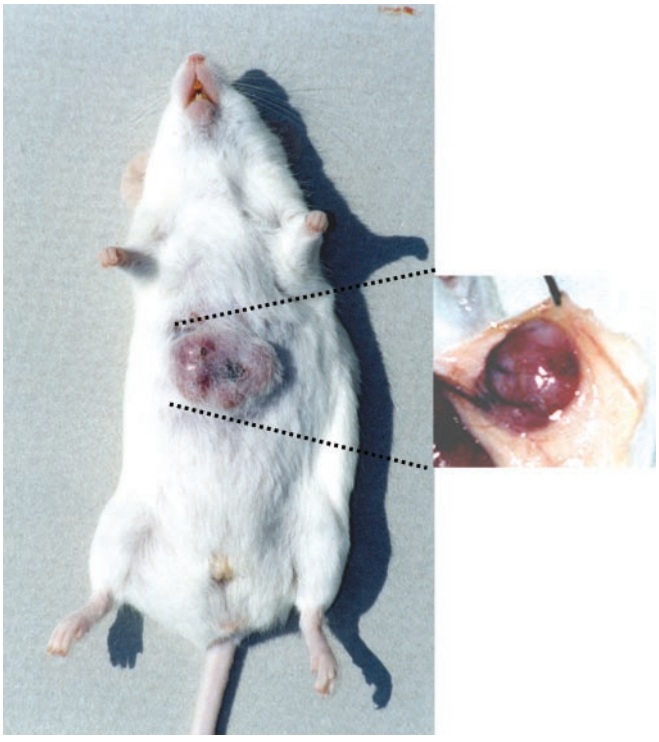

Fig. 2. Grossly visible cutaneous tumor in an irradiated *Ptch1*$^{neo67/+}$ heterozygote. The tumor was locally aggressive but completely circumscribed into the skin.

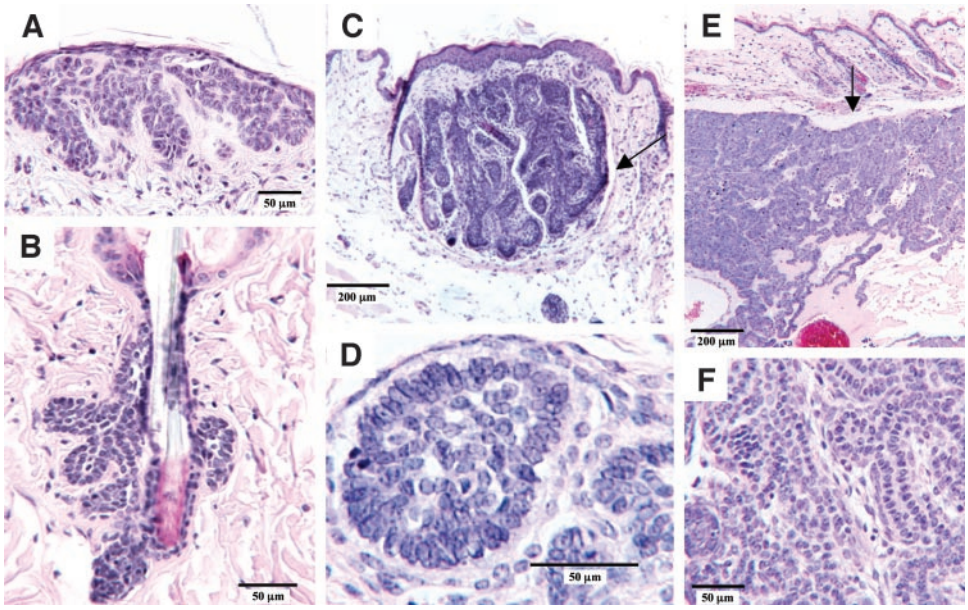

Fig. 3. Histological features of basal cell carcinoma (BCC)-like tumors of different developmental stages in X-ray-irradiated *Ptch1*$^{neo67/+}$ heterozygous mice. Hyperproliferation areas of basaloid cells were associated with interfollicular (*A*) or follicular epidermis (*B*). Nodular BCC-like tumor circumscribed into the dermis. Note the cleft between normal dermis and tumor stroma (→; *C*). Higher magnification of tumor in *B:* cell cluster with typical peripheral palisading pattern (*D*). Infiltrative BCC-like tumor characterized by an aggressive growth pattern. The tumor deeply infiltrates below the dermis. Cleft between normal dermis and tumor stroma (→; *E*). Basaloid cell nests of infiltrative BCC-like tumor show the typical peripheral cell palisading (*F*).

The major causes of death were medulloblastoma and thymic lymphoma (15). Irradiated *Ptch1*$^{neo67/+}$ mice developed large cutaneous tumors that were classified as infiltrative BCCs, appearing as translucent scarlet papules often superficially ulcerated (Fig. 2).

Unirradiated Skin. In the normally appearing skin of *Ptch1*$^{neo67/+}$ heterozygotes, histological examination showed the presence of microscopic basaloid hyperproliferation areas in which cells showed loss of normal polarity, projecting down into the dermis at interfollicular sites (IH; Fig. 3*A*) or in association with hair follicles (FH; Fig. 3*B*). Cells in the follicular/interfollicular buds were characterized by small nuclei and scant cytoplasm, the typical features of elements of the basal compartment. Hyperproliferation areas were detected in 27% of *Ptch1*$^{neo67/+}$ heterozygous mice (Table 2). These microscopic lesions could only be detected by microscopic examination of the skin performed at mouse death; thus, their time of onset could not be precisely determined. However, most of them were diagnosed in mice older than 1 year (mean age: 75 weeks). These small hyperproliferations of basaloid cells were not observed in wild type mice.

Irradiated Skin. The skin of irradiated *Ptch1*$^{neo67/+}$ heterozygotes was macroscopically indistinguishable from that of irradiated wild-type mice, except for the late onset of large BCCs in irradiated mice only (Fig. 2).

Enhancement of Microscopic Hyperproliferations of Basaloid Cells by Radiation. None of the wild-type mice exposed to radiation developed basaloid cell hyperproliferations. In *Ptch1*$^{neo67/+}$ heterozygotes, in contrast, exposure to X-rays resulted in a significant increase in the percentage of mice with small basaloid hyperproliferations, whose incidence raised from 27 to 53–63% ($P < 0.05$), depending on irradiation group. A reduction in the mean age of *Ptch1*$^{neo67/+}$ mice with basaloid hyperproliferations was also observed after irradiation (mean age: 50 weeks). The incidence of hyperproliferation areas in the different groups is given in Table 2.

Induction of Nodular BCCs. *Ptch1*$^{neo67/+}$ heterozygotes exposed to a single dose of ionizing radiation developed skin tumors with histological features of nodular human BCCs that were absent in the skin of unirradiated heterozygotes. Microscopically detectable nodular BCC-like tumors were well-circumscribed, entirely intradermic nodules of variable size and shape, showing the presence of nests of basaloid cells with peripheral palisading (Fig. 3, *C* and *D*). Connection with the epidermis and/or the hair follicle was often observed. The overlaying epidermis was frequently thickened and hyperplastic. The incidence of nodular lesions ranged from 21 to 47% in the different irradiation groups (Table 2). Tumor multiplicities determined on mice surviving 60–90 weeks after irradiation were 8.5 ± 2.9 and 2.4 ± 0.8 in the 3 Gy–90 days and 4 Gy groups, respectively. Although for both parameters there was a trend toward an increased effectiveness in mice irradiated whole body with 3 Gy X-rays at 90 days, these differences were not statistically significant. Tumor multiplicity was not calculated in the 3 Gy neonatal irradiation group because almost all mice died before 60 weeks of age.

Although we could not determine tumor latency for nodular BCCs, examination of mice irradiated as newborns, characterized by early mortality, showed that these tumors were detectable 13 weeks postirradiation. Irradiated wild-type mice did not develop nodular BCCs.

Induction of Infiltrative BCCs. Macroscopic tumors with histological features of infiltrating human BCCs were first detected in the skin of irradiated heterozygotes 16 weeks after irradiation. As shown in Table 3, infiltrative BCC-like tumors appeared dorsally or ventrally along the trunk. Unlike the nodular subtype, these macroscopic tumors developed only in male mice. Tumor diameters ranged from 4 to

Table 2 *Incidence of basal cell carcinoma (BCC)-like tumors in Ptch1*$^{neo6/7}$ *heterozygotes*

	Microscopic basal cell lesions			Macroscopic BCC-like tumors	
Irradiation	No. of mice autopsied	Mice with IH/FH[a] (%)	Mice with nodular BCCs (%)	No. of mice	Mice with macroscopic BCCs (%)
3 Gy neonatal	46	29 (63.0)[b]	11 (23.9)[b]	52	2 (3.8)
3 Gy adult	32	17 (53.1)[b]	15 (46.9)[b]	33	4 (12.1)[b]
4 Gy adult	47	29 (61.7)[b]	10 (21.3)[b]	61	3 (4.9)
None	33	9 (27.3)		52	

[a] Interfollicular/follicular hyperproliferation areas.
[b] Significantly different from unirradiated Ptch1$^{neo67/+}$ mice ($P < 0.05$, Fisher's exact test).

Table 3 *Infiltrative BCC-like tumors in Ptch1$^{neo6/7}$ heterozygotes*

Irradiation	Weeks of latency (tumor code)	Position	Diameter (mm)
3 Gy neonatal	75 (1)	Dorsal	8
	16 (2)	Dorsal	7
3 Gy adult	31 (3)	Ventral	7
	38 (4)	Dorsal	13
	71 (5)	Dorsal	10
	26 (6)	Dorsal	5
4 Gy adult	32 (7)	Ventral	15
	45 (8)	Ventral	4
	77 (9)	Ventral	8

15 mm. Incidences of infiltrative BCCs in the various groups (Table 2) were essentially in agreement with the pattern observed for nodular tumors. BCC incidence in the 3 Gy–90 days group was 12.1%, *i.e.*, 2.5 times higher compared with the incidence of 4.9% observed in the 4 Gy group. Although this difference was not statistically significant, a trend toward an increased effectiveness in mice irradiated whole body with 3 Gy X-rays at 90 days was confirmed for infiltrative BCCs. Irradiation of neonatal mice resulted in a low incidence of infiltrative BCCs (3.8%) because of early mortality in this group. Infiltrative BCCs showed a late onset with a mean latency of 46 weeks. The kinetics of induction of infiltrative BCCs in the different groups is reported in Fig. 4.

Microscopic examination of these large tumors showed a locally aggressive growth pattern, although they did not invade the muscle. The histological features showed dense tumor nodules with margins characterized by cylindrical tumor cell chains arranged in a palisade pattern (Fig. 3*F*). The presence of clefts between tumor stroma and normal dermis was observed (Fig. 3*E*). Infiltrative BCC-like tumors were neither observed in irradiated wild-type mice, nor in unirradiated heterozygotes. No squamous cell carcinomas were induced by irradiation.

BCC Origin and Shh Signaling. To confirm the basal cell origin of skin tumors, we used K14 as a basal differentiation marker. In normal skin, the basal cell layer of the epidermis, the outer root sheath, and the sebaceous glands displayed marked immunoreactivity for anti-K14 antibody (Fig. 5*A*). No immunoreactivity was detected in the remaining follicular compartments such as the inner root sheath and the bulb. Basaloid hyperproliferation areas, as well as nodular and infiltrative BCCs, showed strong immunoreactivity for anti-K14 antibody, suggesting a common progenitor for all basal cell lesions observed (Fig. 5, *B–D*).

Because Ptch1 expression is induced by Shh, we used an anti-Ptch1 antibody to establish activation of the Shh pathway in the skin of *Ptch1$^{neo67/+}$* heterozygous mice. A strong Ptch1 immunoreactivity was detected in the outer root sheath of hair follicles during anagen (Fig. 6*A*), indicating that this phase is dependent on Shh pathway expression. Strong Ptch1 expression was also observed in basal cell hyperproliferation areas and nodular BCC-like tumors during anagen (Fig. 6, *A* and *B*). No Ptch1 expression was detected in the epidermal basal compartment, hyperproliferation areas, and nodular BCC-like tumors during telogen, the resting phase of hair cycle (Fig. 6, *C* and *D*), supporting the notion of temporal control of Shh pathway expression during postnatal hair follicle growth.

p53 Protein Expression in BCC Subtypes. We performed immunohistochemical analysis to look for evidence of p53 immunoreactivity in basaloid hyperproliferation areas and in ionizing radiation-induced nodular and infiltrative BCCs. Basaloid hyperproliferation areas (10 of 10), as well as the normal skin, showed negative p53 staining (Fig. 7*A*). In contrast, analysis of radiation induced nodular and infiltrative BCCs showed an intense, dispersed pattern of p53 protein expression in 88% (7 of 8) of nodular and 100% (7 of 7) of infiltrative BCCs (Fig. 7, *B* and *C*), suggesting a possible involvement of p53 in the formation of these tumors. The intensity of overall staining was similar in nodular and infiltrative subtypes.

Analysis of *Ptch1* Allelic Status. The *Ptch1* allelic status was examined in 10 microdissected nodular BCC-like tumors and matching normal skin tissues. Retention of the wild-type *Ptch1* allele was detected in all tumors examined. A representative agarose gel set is shown in Fig. 8*A*. All infiltrative BCCs developed in these experiments were examined for their allelic status at the *Ptch1* locus. Fig. 8*B* shows loss of the wild-type *Ptch1* allele in 100% of infiltrative BCCs (9 of 9).

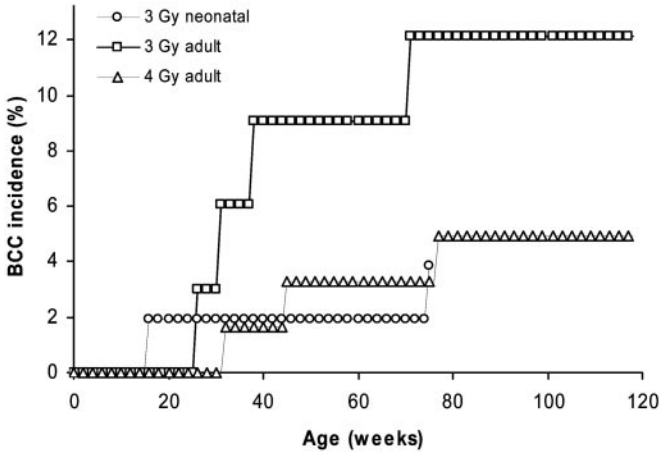

Fig. 4. Incidence of infiltrative basal cell carcinoma (BCC)-like tumors in X-ray-irradiated *Ptch1$^{neo67/+}$* heterozygous mice. The highest BCC incidence was observed in the 3 Gy group irradiated as adults (12.1%). A 4% BCC incidence was observed in neonatally irradiated mice at 75 weeks after irradiation. Mice irradiated with 4 Gy showed a 4.9% BCC incidence. No BCCs were observed in unirradiated mice.

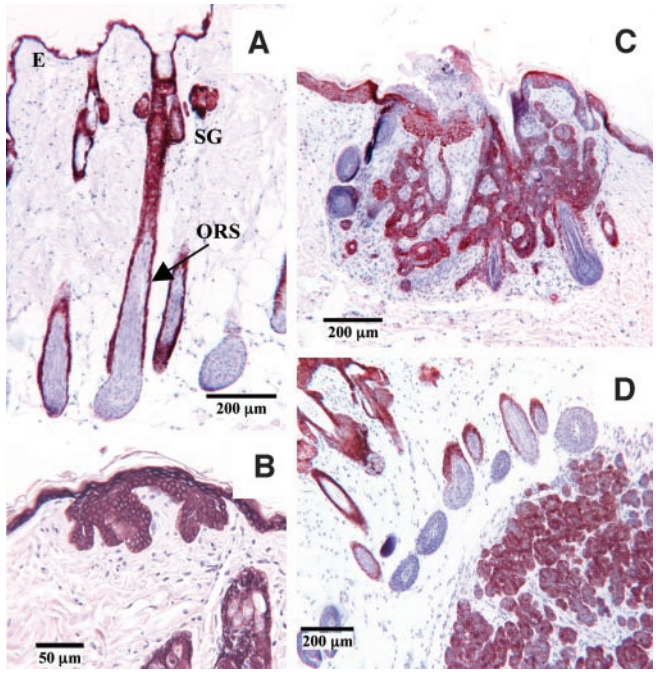

Fig. 5. Anti-CK14-staining of skin lesions. In the normal skin, a strong immunoreactivity is present in the epidermis (E), outer root sheath (ORS), and sebaceous glands (SG; *A*). Similarly, hyperproliferation areas (*B*), nodular BCCs (*C*), and infiltrative BCC-like tumors (*D*) show strong immunoreactivity after incubation with anti-K14 antibody, confirming their basal origin.

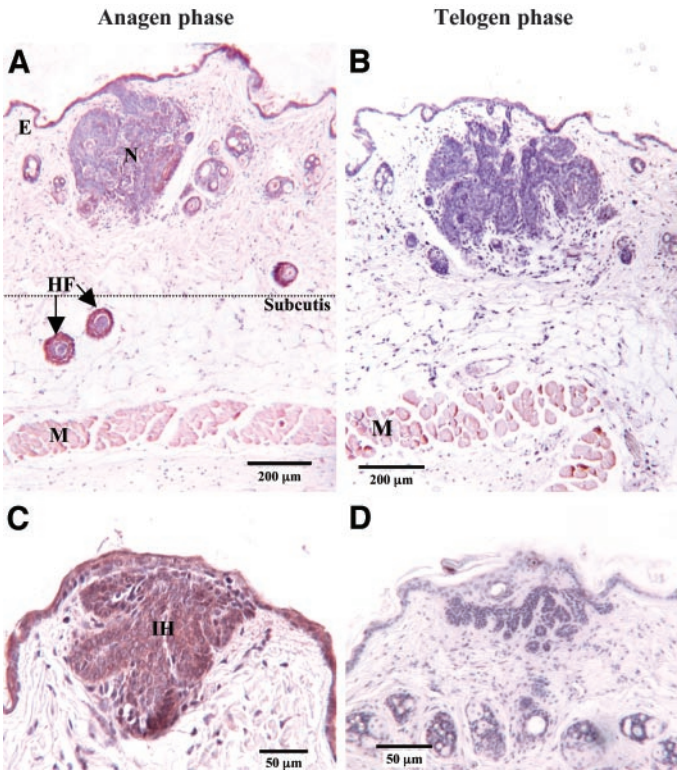

Fig. 6. Immunohistochemical characterization of skin lesions using anti-Ptch1 antibody at different stages of hair growth. *A* and *B*, during anagen phase, identified by the presence of hair follicle into the subcutis, immunoreactivity was detectable in the epidermis (E), hair follicles (HF), interfollicular hyperproliferation areas (IH), nodular BCC-like tumors (N), and muscular tissue (M). *C* and *D*, during telogen phase, characterized by the absence of follicles into the subcutis, Ptch1 immunoreactivity is restricted to the muscular tissue (M).

DISCUSSION

The principal etiologic factors in human BCC tumorigenesis include UV and ionizing radiation, chemical carcinogens, and possibly infection with human papillomaviruses (17). Especially in BCNS patients, BCCs occur with greater incidence in portals of radiotherapy, indicating ionizing radiation as a common *Ptch1* mutagen. Inherent resistance of the mouse to BCC induction by mutagenic chemicals and UV or ionizing radiation has hampered progress in understanding the mechanisms underlying BCC development. *Ptch1* heterozygous knockout mice have provided a new tool for the study of UV- and ionizing radiation-induced BCC tumorigenesis (16).

To clarify the mechanisms by which ionizing radiation induce BCC development, control and irradiated *Ptch1*$^{neo67/+}$ mice and wild-type littermates were monitored for their whole life span. Particular attention was paid to skin abnormalities, and skin samples were analyzed at mouse death. The skin of unirradiated *Ptch1*$^{neo67/+}$ mice was macroscopically normal, and only microscopic examination showed the presence of hyperproliferations of basaloid cells arising from both the hair follicles and the interfollicular epithelium. These occurred in ~25% of mice.

The interaction of ionizing radiation with *Ptch1* deficiency resulted in a strong alteration of the skin phenotype. Development of basaloid hyperproliferation areas (Fig. 3, *A* and *B*) was enhanced by X-rays, and their incidence increased to 53–63% depending on irradiation group. No difference in morphology was observed in microscopic lesions from unirradiated or irradiated mice. In addition, the skin of irradiated *Ptch1*$^{neo67/+}$ heterozygous mice showed the occurrence of microscopically detectable, intradermal, well-circumscribed nodular BCCs (Fig. 3, *C* and *D*), as well as of large infiltrative BCC-like tumors (Figs. 2 and 3, *E* and *F*). Neither of the last two histological subtypes was found in unirradiated *Ptch1*$^{neo67/+}$ heterozygotes, demonstrating a direct causal relationship between ionizing radiation exposure and BCC development.

Deregulation of the Shh pathway has been closely linked to BCC

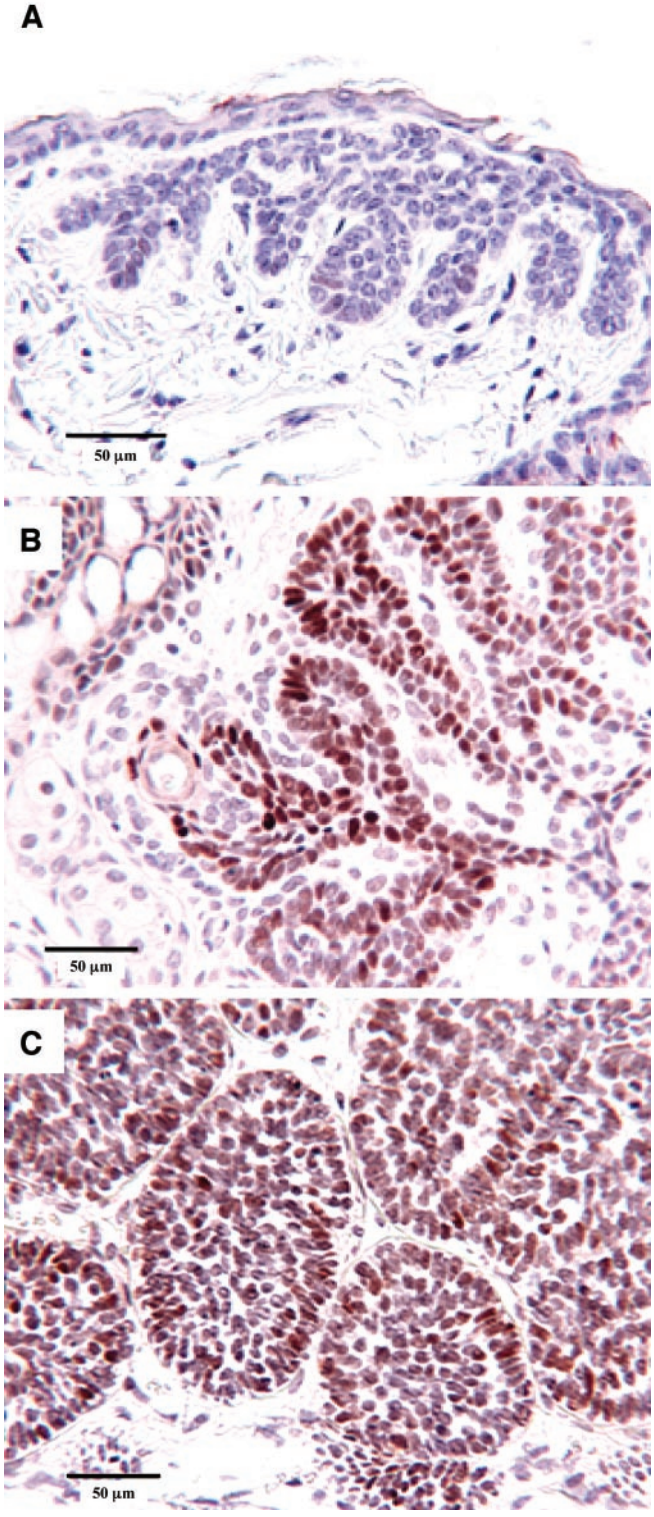

Fig. 7. Expression of p53 in *Ptch1*$^{neo67/+}$ mouse skin and tumors. *A*, negative immunoreactivity for p53 in interfollicular basaloid hyperproliferation and normal skin. *B*, p53 is expressed in a radiation-induced nodular BCC mainly in peripheral cells but not in normal skin. *C*, pattern of p53 protein expression in infiltrative BCC, showing peripheral staining of tumor nests.

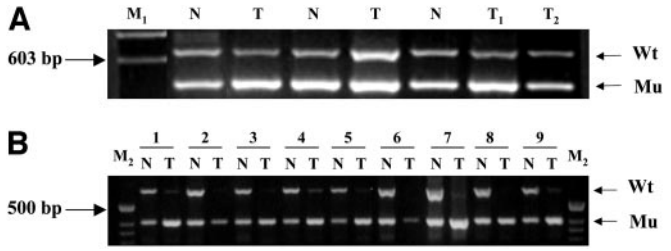

Fig. 8. Analysis of *Ptch1* allelic status in nodular and infiltrative basal cell carcinoma (BCC)-like tumors. DNA extracted from normal (N) and tumor tissue (T) was examined for allelic status of *Ptch1* locus. *A*, representative set of amplified DNAs obtained from nodular BCC-like tumors by microdissection. The wild-type *Ptch1* allele is retained in all tumors. (T_1 and T_2 = two different nodular BCCs from the same mouse). *B*, all infiltrative BCC-like tumors show loss of wild-type *Ptch1*. M_1, marker (Phix *Hae*III fragments-LT 1 bp); M_2, 1 Kb DNA ladder (Invitrogen, Carlsbad, CA).

development, but the mechanisms of BCC tumorigenesis have not been completely clarified yet. As shown by microscopic skin alterations in unirradiated *Ptch1*$^{+/-}$ mice, deregulation of the Shh-Ptch pathway represents the initiating step in BCC development and constitutes a rate-limiting event in BCC formation. However, it is not by itself sufficient for full BCC development in *Ptch1*$^{+/-}$ mice (9). Our tumor data from irradiated *Ptch1*$^{neo67/+}$ heterozygotes (Tables 2 and 3) identify hyperproliferation areas as the most frequent type of basal cell lesion, followed by nodular and finally by infiltrative BCCs, the least frequent subtype. In addition, although multiple nodular BCCs developed in each mouse, infiltrative BCCs developed always as solitary tumors. Finally, although our experimental approach did not allow direct determination of the latency for microscopic tumors, our results suggest that nodular BCCs have shorter latency compared with infiltrative BCCs. In mice irradiated neonatally (3 Gy), nodular BCCs appeared as early as 3 months after irradiation, and 7 of 11 independent nodular tumors were detected in mice that died before 6 months of age (data not shown). Instead, infiltrative BCCs showed a delayed onset, with 7 of 9 ionizing radiation-induced tumors developing in mice older than 10 months, paralleling the human situation where BCC is mainly a disease of the elderly. These findings are consistent with the hypothesis of chronological tumor progression from tumor precursor lesions toward overt neoplasias, with epidermal hyperproliferation areas and nodular and infiltrative BCC-like tumors representing different stages of BCC development.

The expression of Shh protein in normal skin is subject to tight spatial and temporal regulation (18, 19), being restricted to cells at the distal portion of the growing hair follicle and to the anagen hair growth phase (20). Shh induces transcription of target genes, including *Ptch1* itself, by antagonizing the activity of Ptch1. Immunohistochemical analysis of *Ptch1*$^{neo67/+}$ skin showed positive Ptch1 staining of the outer root sheath of hair follicles and of microscopic basal cell lesions (*i.e.*, basaloid hyperproliferations and nodular BCCs) only during anagen. In contrast, no Ptch1 staining was observed during telogen-stage skin (Fig. 6), suggesting temporal regulation of Shh signaling in both growing hair follicles and in epidermal hyperproliferation areas and nodular BCCs. These observations are similar to those reported for *Ptch1*$^{+/-}$ mice (exon 1/2; Ref. 19) and suggest that Shh pathway activation in the skin of *Ptch1*$^{neo67/+}$ heterozygotes is still anagen restricted and that haploinsufficiency is not by itself sufficient to cause constitutive activation of the pathway. In contrast, marked up-regulation of *Shh* target genes is a hallmark of full-blown BCC. This suggests that modestly deregulated *Shh* signaling plays a role in the development of basaloid hyperproliferation, but a critical threshold of signaling activity must be achieved for full BCC development. Recent studies have pointed out the importance of the level of hedgehog pathway deregulation in the development of basal cell tumors and the need of high levels of Shh signaling for the sustained, expansive tumor growth characteristic of BCCs (9, 21).

The appearance of nodular and infiltrative BCCs in the skin of irradiated *Ptch1*$^{neo67/+}$ mice suggests that development of these tumors requires additional genetic lesions, consistent with the fact that tumor development is believed to require a number of genetic alterations. In human BCCs, the tumor suppressor gene *p53* is frequently mutated (22, 23), suggesting that *p53* mutations are an early and required event in BCC tumorigenesis. In the mouse, *p53* gene mutations were detected in BCCs induced by long-term UV exposure in *Ptch1*$^{+/-}$ mice (exon 1/2; Ref. 16). Nilsson *et al.* (21), in contrast, failed to detect *p53* mutations in spontaneous BCCs from *K5-Gli-1*-transgenic mice. In this study, immunohistochemical analysis of p53 expression showed intense p53-positive staining in nodular and infiltrative BCC-like tumors but not in hyperproliferation areas (Fig. 7), suggesting that altered *p53* signaling may be a prerequisite also for murine BCC. Surprisingly, there was no correlation between expression level and tumor aggressiveness because the pattern of p53 staining was similar in nodular and infiltrative BCC-like tumors. This contrasts with a study of relation of p53 expression to the aggressive infiltrative histopathological feature of human BCC (24).

BCNS patients inherit one copy of mutated *Ptch1* and develop BCC mainly after exposure to UV or ionizing radiation when the remaining wild-type copy is mutated or deleted in epidermal keratinocytes. Although limited data exist for BCC development in *Ptch1* heterozygous knockout mice, loss of heterozygosity at the *Ptch1* locus after UV or ionizing radiation has been implicated in BCC tumorigenesis (16). We analyzed ionizing radiation-induced infiltrative BCCs for the allelic status at the *Ptch1* locus and detected loss of the wild-type *Ptch1* allele in all infiltrative BCCs examined (9 of 9; Fig. 8*B*). Our results confirm that the *Ptch1* gene is an important target of radiation and that cells lacking both *Ptch1* alleles undergo clonal expansion leading to uncontrolled growth and local invasion. In view of the development of different types of skin lesions in irradiated *Ptch1*$^{neo67/+}$ heterozygotes, we next investigated the status of the wild-type *Ptch1* allele in the nodular, microscopic subtype. Analysis of 10 microdissected nodular BCCs showed retention of the wild-type allele (Fig. 8*A*), indicating that other factors must contribute to this step of neoplastic progression. These results, taken together with the latencies of skin lesion development, suggest that tumor type may be dependent on quality and quantity of additional acquired mutations and that irradiated *Ptch1*$^{neo67/+}$ epidermis is more permissive to accumulation of additional oncogenic mutations, including loss of wild-type *Ptch1*. This may be a consequence of increased genomic instability associated with altered *p53* signaling, which may enhance the rate of acquisition of secondary mutations.

Our results strongly support the hypothesis of a process occurring through the accumulation of genetic alterations reminiscent of that seen in colorectal cancer (25) in which a crucial role has been attributed to mutations activating the Wnt pathway that shares many similarities with the Shh pathway (26). Although the concept of BCC tumorigenesis as a multistep process conflicts with the lack of premalignant lesions reported for BCCs (27), this hypothesis has recently been suggested for human BCC (28).

In contrast to mouse models overexpressing nuclear mediators of Shh signaling (*e.g.*, *K5-Gli-1*-transgenic mice; Ref. 21), showing rapid and frequent appearance of BCC-like growths during late embryogenesis, the frequency of spontaneous basaloid hyperproliferations in *Ptch1*$^{neo67/+}$ mice was relatively low and delayed. Although requirement for additional genetic damage can be postulated even at this early stage, we favor the hypothesis that deregulation of this pathway at a proximal level may be less effective than deregulation at a distal level (*e.g.*, Gli-1, Gli-2; Refs. 21, 29). Consistent with this supposition

is the finding that Shh target gene induction in *Ptch1* heterozygotes maintains normal hair cycle dependence (Fig. 6; Ref. 19), which appears to be a key mechanism for accurate control of morphogenesis and renewal of hair follicle. In keeping with this view, the X-ray-induced enhancement of basaloid hyperproliferations may be due to a Shh-mediated mechanism of tissue repopulation after radiation damage analogous to that operating in the airway epithelium after injury caused by chemical damage (30), rather than being associated with secondary genetic hits.

A surprising outcome of our study was the strong effect of gender on radiation-induced BCC tumorigenesis. Although microscopic basal cell lesions were observed in males and females, infiltrative BCCs only developed in males. Male sex is a known risk factor for BCC also in humans (31) and is associated with more BCC/year (rate ratio: 1.2). Although the role of estrogens in the development of skin cancer is controversial (32), our results point to an effect of hormonal status on BCC development, consistent with recent findings showing that *Ptch1* is involved in the response to steroid hormones such as estrogens and progesterone and also to their precursor, *i.e.*, cholesterol (33, 34). Additional experimentation is needed to consolidate the possibility of involvement of Shh-Ptch1 signaling in hormone-induced susceptibility to BCC development.

An additional important observation is the difference in BCC induction between mice irradiated locally at 60 days and mice irradiated whole body at 90 days. Although not statistically significant, higher incidence of both nodular and infiltrative BCCs were observed in the latter group, which may point to a relationship between radiation susceptibility and age-dependent hair growth cycle phase (35). On the basis of this hypothesis, mice in a growth phase of the hair cycle (90 days) may be more susceptible to BCC induction compared with mice in a resting phase (60 days). This age dependence is likely to reflect the ability of hair progenitor cells to express the hedgehog pathway and proliferate at the time of irradiation (36). Age-dependent susceptibility to BCC induction would imply a strong concordance with the cellular mechanisms of induction of medulloblastoma by ionizing radiation in *Ptch1*$^{neo67/+}$ mice in which a tumorigenic window of sensitivity reflects the time-limited ability of tumor precursor cells to proliferate (15). Alternately, immunosuppression due to whole-body irradiation might contribute to increase BCC risk (37). To discriminate between these two hypotheses, it will be of interest to examine skin tumor development in mice irradiated locally (*a*) in growth phase of the hair cycle, or (*b*) after induction of an artificial growth phase by hair plucking, or (*c*) by administration of chemical inducers. Experiments are presently underway to investigate hair cycle-phase/immunosuppressive effects.

Finally, in this study we show that mouse lines obtained through deletion of exons 6/7 do not show substantial differences in BCC tumorigenesis compared with *Ptch1*$^{+/-}$ (exon 1/2) mice (16). However, whereas a single X-ray dose was able to induce large, infiltrative BCCs in *Ptch1*$^{neo67/+}$ mice (this study), *Ptch1*$^{+/-}$ mice only developed microscopic BCCs. The mouse age at irradiation (60 days) and the low number ($n = 18$) of exposed mice are likely to be responsible of the absence of macroscopic BCCs in the former study. Another potential explanation could be the genetic background on which *Ptch1*$^{+/-}$ mice (exon 1/2) were generated (16).

In summary, we provided evidence that BCC tumorigenesis in *Ptch1*$^{neo67/+}$ heterozygotes occurs in a multistep fashion. Our data regarding incidence, multiplicity, and latency of the different basal cell lesions, as well as the results of our analysis of p53 protein expression and *Ptch1* allelic status in nodular and infiltrative BCCs are consistent with a model in which (*a*) *Ptch1* haploinsufficiency, by causing modest deregulation of the Shh pathway, determines development of BCC precursor lesions, *i.e.*, basaloid hyperproliferation areas in untreated mice during anagen phase, but it is not sufficient to drive full BCC development; (*b*) after direct genetic damage by radiation in genes serving critical functions in the regulation of cell proliferation, apoptosis, response to DNA damage such as *p53*, BCC precursor lesions progress to nodular, intradermic BCCs; (*c*) genomic instability associated with *p53* mutation promotes complete loss of *Ptch1* function, with constitutive activation of the Shh pathway and progression to large, invasive BCCs. This multistep model provides the opportunity to dissect out the molecular events underlying stepwise progression from precursor lesions to full BCC development. Finally, the development of a model in which BCCs develop in mice within the first year of life after a single X-ray exposure provides a useful tool for the study of both the pathogenesis and treatment of this very common human tumor.

REFERENCES

1. Miller, S. J. Biology of basal cell carcinoma (part I). J. Am. Acad. Dermatol., *24:* 1–18, 1991.
2. Gorlin, R. J. Nevoid basal cell carcinoma syndrome. Dermatol. Clin., *13:* 113–125, 1995.
3. Johnson, R. L., Rothman, A. L., Xie, J., Goodrich, L. V., Bare, J. W., Bonifas, J. M., Quinn, A. G., Myers, R. M., Cox, D. R., Epstein, E. H., Jr., and Scott, M. P. Human homolog of patched, a candidate gene for the basal cell nevus syndrome. Science (Wash. DC), *272:* 1668–1671, 1996.
4. Hahn, H., Wicking, C., Zaphiropoulous, P. G., Gailani, M. R., Shanley, S., Chidambaram, A., Vorechovsky, I., Holmberg, E., Unden, A. B., Gillies, S., Negus, K., Smyth, I., Pressman, C., Leffell, D. J., Gerrard, B., Goldstein, A. M., Dean, M., Toftgard, R., Chenevix-Trench, G., Wainwright, B., and Bale, A. E. Mutations of the human homologue of *Drosophila patched* in the nevoid basal cell carcinoma syndrome. Cell, *85:* 841–851, 1996.
5. Gailani, M. E., and Bale, A. E. Developmental genes and cancer role of patched in basal cell carcinoma of the skin. J. Natl. Cancer Inst. (Bethesda), *89:* 1103–1109, 1997.
6. Ingham, P. W. Transducing Hedgehog: the story so far. EMBO J., *17:* 3505–3511, 1998.
7. Xie, J., Murone, M., Luoh, S. M., Ryan, A., Gu, Q., Zhang, C., Bonifas, J. M., Lam, C. W., Hynes, M., Goddard, A., Rosenthal, A., Epstein, E. H., Jr., and de Sauvage, F. J. Activating *Smoothened* mutations in sporadic basal cell carcinoma. Nature (Lond.), *391:* 90–92, 1998.
8. Lacour, J. P. Carcinogenesis of basal cell carcinomas genetics and molecular mechanism. Br. J. Dermatol., *146:* 17–19, 2002.
9. Grachtchouk, V., Grachtchouk, M., Lowe, L., Johnson, T., Wei, L., Wang, A., de Sauvage, F., and Dlugosz, A. A. The magnitude of hedgehog signaling activity defines skin tumor phenotype. EMBO J., *22:* 2741–2751, 2003.
10. Oro, A. E., Higgins, K. M., Hu, Z., Bonifas, J. M., Epstein, E. H., Jr., and Scott, M. Basal cell carcinoma in mice overexpressing sonic hedgehog. Science (Wash. DC), *276:* 817–821, 1997.
11. Sato, N., Leopold, P. L., and Crystal, R. G. Induction of the hair growth phase in postnatal mice by localized transient expression of Sonic hedgehog. J. Clin. Investig., *104:* 855–864, 1999.
12. Jih, D. M., Lyle, S., Elenitsas, R., Elder, D. E., and Cotsarelis, G. Cytokeratin 15 expression in trichoepitheliomas and a subset of basal cell carcinomas suggests they originate from hair follicle stem cells. J. Cutan. Pathol., *26:* 113–118, 1999.
13. Hahn, H., Wojnowski, L., Zimmer, A. M., Hall, J., Miller, G., and Zimmer, A. Rhabdomyosarcomas and radiation hypersensitivity in a mouse model of Gorlin syndrome. Nat. Med., *4:* 619–622, 1998.
14. Goodrich, L. V., Milenkovic, L., Higgins, K. M., and Scott, M. P. Altered neural cell fates and medulloblastoma in mouse patched mutants. Science (Wash. DC), *277:* 1109–1113, 1997.
15. Pazzaglia, S., Mancuso, M., Atkinson, M. J., Tanori, M., Rebessi, S., Di Majo, V., Covelli, V., Hanh, H., and Saran, A. High incidence of medulloblastoma following X-ray irradiation of newborn *Ptch1* heterozygous mice. Oncogene, *21:* 7580–7584, 2002.
16. Aszterbaum, M., Epstein, J., Oro, A., Douglas, V., LeBoit, P. E., Scott, M. P., and Epstein, E. H., Jr. Ultraviolet and ionizing radiation enhance the growth of BCCs and trichoblastomas in patched heterozygous knockout mice. Nat. Med., *5:* 1285–1291, 1999.
17. Bastiaens, M. T., Hoefnagel, J. J., Bruijn, J. A., Westendorp, R. G. J., Vermeer, B. J., and Bouwes Bavinck, J. N. Differences in age, site distribution, and sex between nodular and superficial basal cell carcinoma indicate different types of tumors. J. Investig. Dermatol., *110:* 880–884, 1998.
18. Morgan, B. A., Orkin, R. W., Noramly, S., and Perez, A. Stage-specific effects of sonic hedgehog expression in the epidermis. Dev. Biol., *201:* 1–12, 1998.
19. Oro, A. E., and Higgins, K. Hair cycle regulation of hedgehog signal reception. Dev. Biol., *255:* 238–248, 2003.

20. Gat, U., DasGupta, R., Degenstein, L., and Fuchs, E. *De novo* hair follicle morphogenesis and hair tumors in mice expressing a truncated β-catenin in skin. Cell, *95:* 605–614, 1998.
21. Nilsson, M., Unden, A. B., Krause, D., Malmqwist, U., Raza, K., Zaphiropoulos, P. G., and Toftgard, R. Induction of basal cell carcinomas and trichoepitheliomas in mice overexpressing GLI-1. Proc. Natl. Acad. Sci. USA, *97:* 3438–3443, 2000.
22. Pontén, F., Berg, C., Ahmadian, A., Ren, Z-P., Nistér, M., Lundeberg, J., Uhlén, M., and Pontén, J. Molecular pathology in basal cell cancer with p53 as a genetic marker. Oncogene, *15:* 1059–1067, 1997.
23. Zhang, H., Ping, X. L., Lee, P. K., Wu, X. L., Yao, Y. J., Zhang, M. J., Silvers, D. N., Ratner, D., Malhotra, R., Peacocke, M., and Tsou, H. C. Role of *PTCH* and *p53* genes in early-onset basal cell carcinoma. Am. J. Pathol., *158:* 381–385, 2001.
24. Auepemkiate, S., Boonyaphiphat, P., and Thongsuksai, P. p53 expression related to the aggressive infiltrative histopathological feature of basal cell carcinoma. Histopathology, *40:* 568–573, 2002.
25. Fearon, E. R., and Vogelstein, B. A genetic model for colorectal tumorigenesis. Cell, *61:* 759–767, 1990.
26. Kalderon, D. Similarities between the Hedgehog and Wnt signaling pathways. Trends Cell. Biol., *12:* 523–531, 2002.
27. Brash, D. E., and Ponten, J. Skin precancer. Cancer Surv., *32:* 69–113, 1998.
28. Saldanha, G. The Hedgehog signalling pathway and cancer. J. Pathol., *193:* 427–432, 2001.
29. Grachtchouk, M., Mo, R., Yu, S., Zhang, X., Sasaki, H., Hui, C. C., and Dlugosz, A. A. Basal cell carcinomas in mice overexpressing *Gli2* in skin. Nat. Genet., *24:* 216–217, 2000.
30. Watkins, D. N., Berman, D. M., Burkholder, S. G., Wang, B., Beachy, P. A., and Baylin, S. B. Hedgehog signalling within airway epithelial progenitors and in small-cell lung cancer. Nature (Lond.), *422:* 313–317, 2003.
31. Ramachandran, S., Fryer, A. A., Lovatt, T. J., Smith, A. G., Lear, J. T., Jones, P. W., and Strange, R. C. Combined effects of gender, skin type and polymorphic genes on clinical phenotype: use of rate of increase in numbers of basal cell carcinomas as a model system. Cancer Lett., *189:* 175–181, 2003.
32. Rogers, G. S., Flowers, J. L., Pollack, S. V., and McCarty, K. S., Jr. Determination of sex steroid receptor in human basal cell carcinoma. J. Am. Acad. Dermatol., *18:* 1039–1043, 1988.
33. Chang-Claude, J., Dunning, A., Schnitzbauer, U., Galmbacher, P., Tee, L., Wjst, M., Chalmers, J., Zemzoum, I., Harbeck, N., Pharoah, P. D., and Hahn, H. The patched polymorphism Pro1315Leu (C3944T) may modulate the association between use of oral contraceptives and breast cancer risk. Int. J. Cancer, *6:* 779–783, 2003.
34. Kuwabara, P. E., and Labouesse, M. The sterol-sensing domain: multiple families, a unique role? Trends Genet., *18:* 193–201, 2002.
35. Muller-Rover, S., Handjiski, B., van der Veen, C., Eichmuller, S., Foitzik, K., McKay, I. A., Stenn, K. S., and Paus, R. A comprehensive guide for the accurate classification of murine hair follicles in distinct hair cycle stages. J. Investig. Dermatol., *117:* 3–15, 2001.
36. Callahan, C. A., and Oro, A. E. Monstrous attempts at adnexogenesis: regulating hair follicle progenitors through Sonic hedgehog signaling. Curr. Opin. Genet. Dev., *11:* 541–546, 2001.
37. Rubel, J. R., Milford, E. L., and Abdi, R. Cutaneous neoplasms in renal transplant recipients. Eur. J. Dermatol., *12:* 532–535, 2002.